ChemComm

FEATURE ARTICLE

Curly arrows meet electron density transfers in chemical reaction mechanisms: from electron localization function (ELF) analysis to valence-shell electron-pair repulsion (VSEPR) inspired interpretation

Juan Andrés,[a] Sławomir Berski[b] and Bernard Silvi*[c]

Cite this: DOI: 10.1039/c5cc09816e

Probing the electron density transfers during a chemical reaction can provide important insights, making possible to understand and control chemical reactions. This aim has required extensions of the relationships between the traditional chemical concepts and the quantum mechanical ones. The present work examines the detailed chemical insights that have been generated through 100 years of work worldwide on G. N. Lewis's ground breaking paper on The Atom and the Molecule (Lewis, G. N. The Atom and the Molecule, *J. Am. Chem. Soc.* 1916, **38**, 762–785), with a focus on how the determination of reaction mechanisms can be reached applying the bonding evolution theory (BET), emphasizing how curly arrows meet electron density transfers in chemical reaction mechanisms and how the Lewis structure can be recovered. BET that combines the topological analysis of the electron localization function (ELF) and Thom's catastrophe theory (CT) provides a powerful tool providing insight into molecular mechanisms of chemical rearrangements. In agreement with physical laws and quantum theoretical insights, BET can be considered as an appropriate tool to tackle chemical reactivity with a wide range of possible applications. Likewise, the present approach retrieves the classical curly arrows used to describe the rearrangements of chemical bonds for a given reaction mechanism, providing detailed physical grounds for this type of representation. The ideas underlying the valence-shell-electron pair-repulsion (VSEPR) model applied to non-equilibrium geometries provide simple chemical explanations of density transfers. For a given geometry around a central atom, the arrangement of the electronic domain may comply or not with the VSEPR rules according with the valence shell population of the considered atom. A deformation yields arrangements which are either VSEPR defective (at least a domain is missing to match the VSEPR arrangement corresponding to the geometry of the ligands), VSEPR compliant or pseudo VSEPR when the position of bonding and non-bonding domains are interchanged. VSEPR defective arrangements increase the electrophilic character of the site whereas the VSEPR compliant arrangements anticipate the formation of a new covalent bond. The frequencies of the normal modes which account for the reaction coordinate provide additional information on the succession of the density transfers. This simple model is shown to yield results in very good agreement with those obtained by BET.

Received 30th November 2015,
Accepted 18th May 2016

DOI: 10.1039/c5cc09816e

www.rsc.org/chemcomm

1 Curly arrows in chemistry

Among the legacy of C. K. Ingold is the development of the electronic theory of organic reactions in which the concept of electron displacement plays an important role in the explanation of reactivity and mechanisms.[1–4] This theory is based on the models of electronic structure of Lewis,[5] Langmuir[6–8] and Thomson.[9,10] Ingold considered two kinds of electron displacements: the inductive effect, represented by an arrowed bond symbol (→), in which the electron pair remains bounded in its original octet and the mesomeric effect, denoted by the curved (curly) arrow symbol (↷), characterized by the substitution of one duplet for another in the same atomic octet.[1,2] Whereas the inductive effect is considered by Ingold to account for permanent molecular states, the mesomeric effect can be associated

[a] *Departament de Ciències Experimentals Universitat Jaume I, 12080 Castelló, Spain*
[b] *Faculty of Chemistry, University of Wrocław, Poland*
[c] *Sorbonne Universités, UPMC, Univ Paris 06, UMR 7616, Laboratoire de Chimie Théorique, case courrier 137, 4 place Jussieu, F-75752 Paris, France. E-mail: silvi@lct.jussieu.fr; Fax: +33 14427 5526; Tel: +33 14427 4211*

either with a permanent state or with an activation phenomenon. The curly arrow symbol has been introduced independently by Lapworth[11] who reconsidered Thiele's concept of partial valence and by Kermack and Robinson[12] to explain induced polarity and conjugation effects. The curly arrow of Kermack and Robinson represented the displacement of a single electron instead of that of an electron pair, such as in Ingold's papers,[4] which became the convention universally adopted. The transfer of a single electron is now represented by the curved fish-hook arrow introduced by Budzikiewicz *et al.*[13] The use of curly arrow pushing has been extended to the formation/dissociation of bonds in chemical reactions.

The curly arrow pushing remains fundamental in organic chemistry. It is an essential tool in education which enables explanatory representations of bond cleavages and bond formations occurring during a chemical reaction. It is part of the core chemical language[14,15] as testified by many classical textbooks.[16–20] From an epistemological viewpoint it belongs to the causal account of explanation[21] which traces the causal processes and interactions leading to the event, here the electron transfers which explain the conversion of the reactants into products.

Lewis introduced empirical rules which are still one of the foundations of chemistry today. In practice, chemists think in terms of bonds and electron pairs. The interpretation of reaction mechanisms of organic reactions in terms of curly arrows[22–25] is based on the chemical structures similar to those introduced by Lewis (and thus still called Lewis structures) in which Lewis's electron pairs are associated to individual chemical bonds and they have a particular meaning. In practice, a bond line representation is used for canonical structures whereas full line curly arrows show the transfer of electron pairs accompanying the breaking of bonds and the formation of new bonds. Rather than the displacement of electron pairs the curly arrows show the re-localization of bonds. The tails and heads of the curly arrow indicate chemical bonds that are weakened and strengthened due to loss or gain of valence electron density during the reaction, respectively. Arrow pushing is determined by Occam's razor principle in order to connect the canonical structures of the reactants and the products without considering the evolution of the geometry of the nuclei. This representation appears to be a consequence of the chemical intuition because there is no experimental support for these curly arrows. An enlightening discussion can be found in Henry Rzepa's blog.[26]

Chemists frequently use concepts lacking a clear physical basis that might appear to be arbitrary and vaguely defined.[27] An example of this is the concept of reaction mechanisms. In chemical reactivity, a reaction mechanism is understood as a sequence of elementary steps by which the overall chemical change occurs. It describes in details what takes place at each stage of the chemical transformation, *i.e.* the way in which chemical events take place such as the along the progress of a chemical reaction, for instance bond cleavage and formation processes, electron pair rearrangements, transformation of formally double to simple bonds or *vice versa*, *etc.* From the perspective of quantum mechanics, the difficulty stems on the fact that a proper description of chemical bond can be rooted on a physically observable property. No quantum mechanical "bond operator" exists that would provide a conventional expectation value. The complexity of the electronic structure in the transient regime of emerging or breaking chemical bonds cannot be unambiguously defined in pure quantum theory, and hampers our understanding of how atoms or molecules bind at a most fundamental level. Reaction mechanisms are rather mental representations of an unreachable reality belonging to the level of understanding of chemistry, a level different from that of physics. Chemists consider molecules as consisting of atoms, physicists as systems of interacting electrons and nuclei.

2 Electron density transfers in reaction mechanisms

Quantum chemistry has been extremely useful and successful for the theoretical analysis of chemical reactions and chemical reactivity. It provided explanatory and predictive models which determine the general descriptive scheme of chemical structures and the fundamental aspects of reactivity. The frontier orbital theory[28] and the orbital symmetry rules of Woodward and Hoffman[29] are paradigmatic examples of the possibilities of quantum chemistry within the molecular orbital (MO) theory. In this sense, MOs allows define a chemical bond, assigned to a pair of electrons shared by two or more nuclei, as put forward by Lewis.[5] Further, in the valence bond (VB) theory account developed by Pauling[30–33] the superposition of resonant Lewis structures represents the chemical bonds by localized electron pairs, providing interpretations on the very nature of bonds, the structure of the molecules, and even of their reactivity.[34,35] In fact, Pauling in his classic paper on the electron pair bond noted that VB theory is the mathematical foundation for Lewis' ideas about the electronic structure of molecules.[5,36] The conceptual density functional (CDF) theory pioneered by R. G. Parr[37,38] is at the origin of very useful reactivity descriptors[39] whereas a general model for transition states proposed by Shaik[40] is currently successfully applied to many areas of chemical reactivity.[34] The attempts made so far to extract the flow and electron transfer processes along the reaction pathway associated to a chemical reaction from quantum chemical calculations are based either on wave function-based and orbital-based methods or on the topology of scalar fields associated to the electron density distributions. The former methods rely by construction on the choice of the expansion technique used to calculate the approximate wave function whereas the topological approach is, in its principles, free of arbitrariness. The localized orbital centroid evolution technique of Leroy *et al.*,[41] the intrinsic bond orbitals transformations[42] and the valence bond approaches used by Karadakov[43] and by Harcourt[44] belong to the former group. The molecular electrostatic potential (MESP) topography approach of Balanarayan *et al.*[45] is very attractive although the

correspondences between the evolution of the MESP and the charge density transfers are stated rather than rigorously established. One step further is based on the idea that the existence of a chemical bond must be related to some observable; in other words, chemical bonding must have an effect on measurable properties of the system. The electron density, $\rho(\mathbf{r})$ is certainly the best choice because it is a local function defined within the exact many body theory which can also be extracted from experimental data. $\rho(\mathbf{r})$ can be calculated by means of first principles methods, *e.g.*, density functional theory, while the total charge density can also be measured *via* X-ray diffraction techniques, and the spin-polarized charge density can be determined using spin-polarized neutron diffraction. From a quantum perspective, the importance of $\rho(\mathbf{r})$, as a fundamental property of an electronic system containing all information of physical relevance, is highlighted by the Hohenberg–Kohn theorem,[46] *i.e.* all ground state properties depend on the charge density. It seems appropriate to seek relationships between the structure of $\rho(\mathbf{r})$, changes to that structure, and corresponding changes to properties.

Therefore, in the deeper study of chemical reactivity, we want to identify how electron density transfers occur as a function of reaction progress. In doing so, we can provide a connection between the $\rho(\mathbf{r})$ distribution and the chemical reactivity. The density distribution $\rho(\mathbf{r})$ of a molecule contains information not only on the atomic structure and electronic properties but also on the nature of the chemical bonds that lead ultimately to chemical reactivity. Recently, Stalke[47] has provided an introduction to the basics of $\rho(\mathbf{r})$ investigations from a theoretical point of view, while Chopra[48] has emphasized the advances in understanding of chemical bonding from experimental and theoretical charge density analysis. The name of quantum chemical topology[49,50] has been introduced to embrace all topological investigations of three-dimensional scalar fields[51–58] to rationalize the chemical bond and further understanding of the chemical reactivity.[59–67] A number of excellent works in the subject have been published to remark the importance of charge density analysis applied to chemical and biological systems and solids.[47,48,56,68–74]

Probing the electron density distribution during a chemical reaction can provide important insights, but this aim has required extension of the relationships between the traditional chemical concepts and the quantum mechanical ones. In this context, the catastrophe theory has been used to study the evolution along a reaction path of the topologies of the electron density,[75,76] the laplacian of the electron density[77] 3 and of the electron localization function (ELF),[78] *i.e.* bonding evolution theory (BET).[78] BET analysis shows a connection between quantum mechanics and bond making/forming processes, and is capable to quantify the transfers of electron density and thus to deduce the accompanying electron flow. In particular, BET retrieves the classical curly arrows used to describe the rearrangements of chemical bonds for a given reaction mechanism, providing detailed physical grounds for this type of representation.[79–83]

A successive detection of the electron density changes along a chemical reaction, in which a continuous redistribution of $\rho(\mathbf{r})$ proceeds, can provide valuable information on the interconnection of the structure of the charge density distribution and the nuclear geometry. This paper, as a tribute to the centenary of the publication of G. N. Lewis' ground breaking paper on The Atom and the Molecule,[5] presents a short review of determination of reaction mechanisms by the BET procedure with the goal to reconcile how curly arrows meet electron density transfers in chemical reaction mechanisms. Thus, questions such as how could the electronic density transfer processes proceed along the reaction path, *i.e.* how is the electronic density flow, in which direction, and how and where the chemical events take place along the reaction pathway may be answered. This combined method that we use herein has been described in much detail previously.[62,78,81,82] It is shown that they can often be predicted by simple chemical rules considering the nuclear geometries along a reaction pathway which are inspired of the valence shell electron pair repulsion (VSEPR) model.[84–86]

3 A sketch of the ELF analysis and of its application to chemical reactions

The essential assumption of the Lewis's model is that it is possible to identify groups of electrons spatially distributed in an atom or a molecule. Different techniques can be used in order to check the falsifiability of this hypothesis. A first group of methods aims to determine the regions of space which maximize the probability of finding a given number of electrons. In the loge theory[87–89] the space is divided in connected non overlapping volumes within which the probability P_ν of finding ν and only ν electrons of given spins is evaluated. The difficulty of finding the loge boundaries has hampered the development of this method. The efficient recurrence formula derived by Cancès *et al.*[90] for single determinantal wave functions has been used to optimize the shape of maximum probability domains (MPDs) which are allowed to overlap. The method has been applied to linear molecules[91] and other simple systems[92–99] and solids.[100] For $\nu = 2$, the MPDs can be associated to cores, bonds and lone pairs when the investigated system is well described by a single Lewis structure. However, the MPDs are not necessarily unique. The method may yield different solutions depending of the initial guess, for example in the FHF^- complex two symmetry related overlapping domains containing the proton correspond to the two F−H bonds. The overlap of these domains is interpreted as being due to the resonance of the $[F–H + F^-]$ and $[F^- + HF]$ structures.

Another approach intends to determine space-filling non overlapping regions, say Ω_A, within which the fluctuation of the population of Ω_A, *i.e.* integrated density over Ω_A,

$$\bar{N}(\Omega_A) = \int_{\Omega_A} \rho(\mathbf{r}) d\mathbf{r}$$

In other words for each region we seek the boundaries for which the variance of (Ω_A) is minimal. The variance can be expressed as the expectation value of the variance

operator,[101,102] which yields a rather simple expression in terms of the integrals of the one-electron density $\rho(\mathbf{r})$ and pair density $\Pi(\mathbf{r},\mathbf{r}')$ over Ω_A:

$$\sigma^2(\bar{N}(\Omega_A)) = \int_{\Omega_A}\int_{\Omega_A} \Pi(\mathbf{r},\mathbf{r}')d\mathbf{r}d\mathbf{r}' - \bar{N}^2(\Omega_A) + \bar{N}(\Omega_A) \quad (1)$$

It follows from eqn (1) that $\sigma^2(\bar{N}(\Omega_A)) = 0$ is satisfied for whole systems, perfectly localized opposite spin electron pairs or single electrons. The minimization of the variance with respect to the domain volumes implies that the variational equation

$$\frac{\delta\sigma^2(\bar{N}(\Omega))}{\delta V(\Omega)} = 0 \quad (2)$$

should be satisfied. This equation can be written in terms of a surface integral

$$\frac{\delta\sigma^2(\bar{N}(\Omega))}{\delta V(\Omega)} = \oint_{S(\Omega)} \mathbf{n}\cdot\nabla\eta(\mathbf{r})ds = 0 \quad (3)$$

in which $\eta(\mathbf{r})$ is a scalar function for which the bounding surface $S(\Omega)$ is a zero flux surface. The determination of $\eta(\mathbf{r})$ from the expression of $\sigma^2(\bar{N}(\Omega))$ is hampered by the fact that it involves a six dimensional integral.[103] Paul W. Ayers has introduced the local covariance measure function to minimize the Frobenius norm of the covariance matrix of the domain populations.[104] This function can be approximated by the kernel of the electron localization function (ELF) of Becke ans Edgecombe.[105] This statement is supported by calculations on atoms[103,106] which show that the shell boundaries calculated by ELF and by the minimization of the variance of the shell populations almost coincide. In molecules, small variations of the basins bounding surfaces off their ELF position increases the variance of the population. The MPDs and the ELF basins are often close one another, except when the MPD approach former approach yields different solutions corresponding to resonant forms[92,107] which are averaged in the ELF partition.

The ELF partition is carried out in the framework of the dynamical system theory[108] and yields basins of attractors which "correspond to the qualitative electron pair domains of the VSEPR model and have the same geometry as the VSEPR domains"[109] and therefore match the Lewis's picture of the bonding. The core basins are labeled as C(A) where A is the atomic symbol of the element. They surround nuclei with atomic charge $Z > 2$. The valence basins, which correspond to bonds and lone pairs, are characterized by their synaptic order which is the number of atomic valence shell to which they belong.[110] There are therefore monosynaptic basins V(A) for lone pairs, disynaptic V(A,B) for two-center bonds and higher polysynaptic basins, V(A,B,C,...) for multicenter bonds. In practice the Born–Oppenheimer approximation is assumed and, therefore, the ELF gradient field depends on the nuclear coordinates which forms the control parameters space and its topology is expressed by its critical points (*i.e.* the points for which $\nabla ELF(\mathbf{r}_c) = 0$) and their connectivity. The set of points of the control parameter space preserving a given topology is called structural stability domain. Along a reaction pathway, a classical trajectory of the nuclei defined by the intrinsic reaction coordinate (IRC),[111–115] the system visits the different stability domains which link the structure of the reactants to that of the product. The transitions between successive structural stability domains occurs at turning points of the control parameter space are described in terms of bifurcation catastrophes in the sense of René Thom.[116] The process of the creation-annihilation of electronic domains depicted by ELF has been formalized in the bonding evolution theory (BET) of Krokidis *et al.*[78] This method has been widely applied to investigate many chemical reactions such as proton transfers,[117–119] electron transfers,[120] hydrogen transfers,[121] oxygen transfers,[122] isomerizations,[79,123–129] reactions of metals and metal oxides with organic and inorganic molecules[130–138] cycloadditions[62,139–147] nucleophilic substitution[148] phase transition in solids.[149,150]

4 How BET procedure reveals electron density transfers

The objective of this study is to characterize the reaction mechanism of chemical reaction through the identification and characterization of the chemical events that drive the reaction by using BET procedure. Chemical events are bond breaking/forming processes, the weakening or strengthening of a chemical bond, the rearrangements or formation/disappearance of electron pairs, *etc.* BET analysis shows a connection between quantum mechanics, bond making/forming process and is capable to quantify the transfers of electron density and therefore to deduce the accompanying electron flows and present approach retrieves the classical curly arrows used to describe the rearrangements of chemical bonds for a given reaction mechanisms, providing detailed physical grounds for this type of representation. The first step is the determination of the intrinsic reaction coordinate (IRC) to connect the stationary points on the potential energy surface (reactants, possible intermediates, transition states, and products). At each point of the IRC a full ELF analysis is carried out which yields the different basins and their populations. The turning points between successive SSDs are localized as they correspond to changes in the number of basins or in their nature. The graph of the basin population along the IRC enables further to identify the electron density transfers, *i.e.* the density flows. The capability of this method is exemplified in the cyclization of buta-1,3-diene.

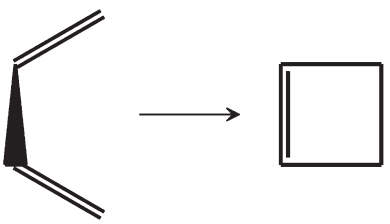

The "*cis*" buta-1,3-diene is in fact a gauche conformer of C_4H_6, as shown by Chattaraj *et al.*[151] It is not planar and has a C_2 symmetry. This implies that the reaction mechanism this

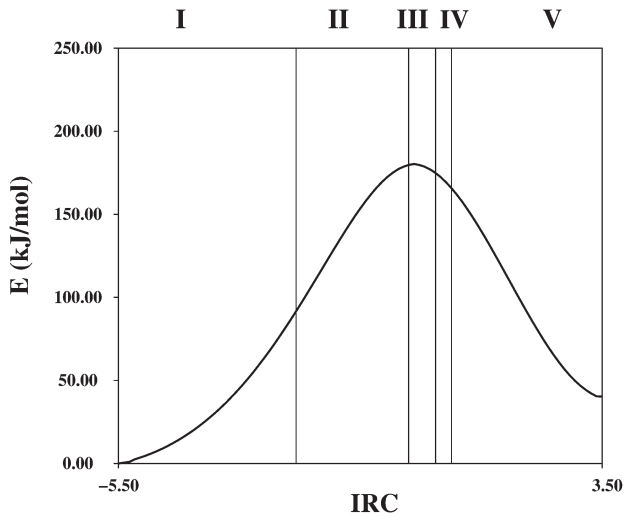

Fig. 1 Energy profile of the cyclization of 1,3 butadiene along the IRC pathway. The vertical lines materialize the structural stability domains boundaries.

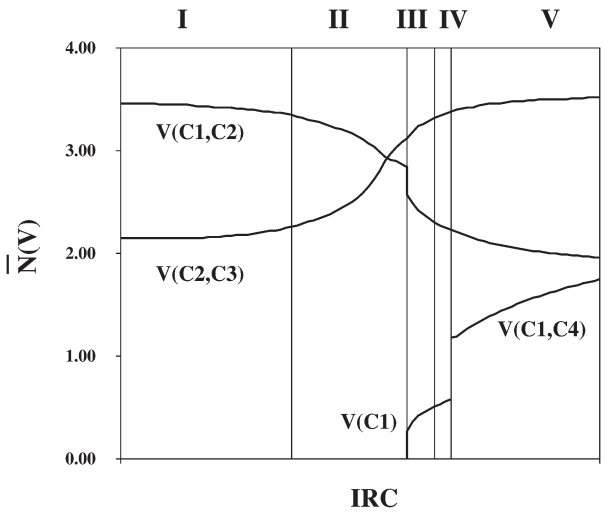

Fig. 2 Basin populations along the IRC pathway. The populations of the double bond basins V_1(C1,C2), V_2(C1,C2) in SSD-I and of V_1(C1,C4), V_2(C1,C4) in SSD-IV and SSD-V have been added. The vertical lines materialize the structural stability domains boundaries. Atom are numbered according to IUPAC conventions.

electrocyclic rearrangement must preserve the C_2 symmetry which implies a conrotatory pathway. The energy profile for the cyclization of buta-1,3-diene along the IRC is displayed in Fig. 1. The first structural stability domain (SSD-I) corresponds to the canonical structure of 1,3 butadiene with one basin V(C2,C3) accounting for the single bond and two pair of basins V_1(C1,C2), V_2(C1,C2) and V_1(C3,C4), V_2(C3,C4). At the first turning point, each pair merges into a single basin. The main nuclear geometry change is the lengthening of the C1–C2 and C3–C4 bonds coupled with the shortening of the C2–C3 bond, a nuclear motion accounted for by the A stretching mode calculated at *ca.* 1700 cm^{-1}. Along the IRC pathway belonging to SSD-II, the two CH_2 groups symmetrically rotate of about 40° around the C1–C2 and C3–C4 bonds which correspond to the A twisting mode at *ca.* 750–1700 cm^{-1}. Just before the transition state, the system evolves to SSD-III where two monosynaptic basins V(C1) and V(C4) appear at the top of the C1 and C4 atoms correlated with the symmetric wagging of the methylene groups. The next event splits the attractor of the inner C–C bond to yield a double bond. Finally, V(C1) and V(C4) merge into V(C1,C4) achieving the closure of the cycle. The evolution of the basin populations presented in Fig. 2 enable to understand the electron density transfers.

The overall charge transfer from V(C1,C2) and V(C3,C4) towards V(C2,C3) is 1.37 e^-, *i.e.* 0.68 e^- from each double bond, whereas the population of the V(C1,C4) basin amounts 1.76 e^- in cyclobutene implying to partial transfers of 0.88 e^-. Rounding to the nearest integer yields a representation in terms of curly fish-hook arrows as:

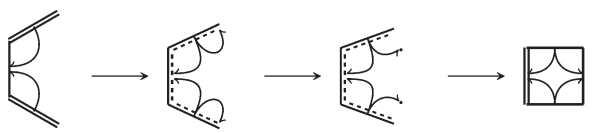

rather than the transfer of an electron, a curly fish-hook arrow, as the dot apart the terminal carbons of the third structure, means the transfer of half an opposite spin pair of integrated density. This example clearly shows the interdependence of electron transfers and geometrical deformations which comply with chemical intuition, for instance the increase of bond length corresponds to a density transfer toward an adjacent bond which is shortened.

5 Electron density transfers and molecular geometry deformations

The electron density transfers observed along the reaction pathway are always correlated with the deformations of the molecular geometry. In a given SSD, they imply valence basins belonging to the valence shell of a common atom. At the turning points between successive SSDs along the reaction pathway density transfers processes may take place and they must be initiated toward new basins or stopped when the annihilation of a basin occurs. In most BET studies, for a system of N_A atoms, the control space consists of the set of $3N_A - 6$, or $3N_A - 5$ if the system is linear, independent nuclear coordinates which can be expressed in terms of internal coordinates. Each turning point is associated to a catastrophe which is described by its universal unfolding, a model mathematical expression describing the behaviour of the system in the neighbourhood of the turning point. The parameters of the universal unfolding indicate how many and which control space parameters are responsible for the catastrophe. The survey of the data collected in BET studies, indicates that, for a given local electronic structure, the same type of catastrophes can be associated to chemical events, corresponding to the same type of deformation of the molecular geometry and therefore of internal coordinates.

Variation of the bond length is involved in the bond formation or bond cleavage as well as in the change of the bond multiplicity. Both events are described by the cusp catastrophe. Two types of angular deformations, the in plane bending of a 180° bond angle and the out of plane bending, are associated with the formation of a new monosynaptic basin on the top of the central atom by a fold catastrophe. The formation of a dative bond is achieved by an elliptic catastrophe in which a monosynaptic basin, V(A), becomes disynaptic V(A,B). It implies the combination of an out of plane angular deformation of the ligands around atom B and the decrease of the A–B distance. Such reorganizations of the valence basins of a central atom are possible if enough electron density is available within its valence shell. There is a close analogy between the ELF basins and the electronic domains introduced by Gillespie[152] in the context of the VSEPR model. Electron pair domains are defined as a charge cloud which occupies a given region of space and excludes other pairs from this region as a consequence of the Pauli exclusion principles. This electron pair domain version of VSEPR emphasizes the shape and size of the domains rather than the magnitude of their mutual repulsion. In addition to bond and lone pair domains, Gillespie considers single electron domains which are expected to be smaller than an electron pair domain.[86] It is convenient to generalize the electronic domain concept by adopting the following definition: an electronic domain is a non overlapping region of space arising from the Pauli principle and which therefore lowers the probability of finding same spin electrons. This definition relies on the strict interpretation of the antisymmetry principle which only concerns the same spin electrons. It has the advantage to be valid for both the opposite spin pair and single electron domains. As noted by Gillespie and Robinson: ''this function (ELF) exhibits maxima at the most probable positions of localized electron pairs and each maximum is surrounded by a basin in which there is an increased probability of finding an electron pair. These basins correspond to the qualitative electron pair domains of the VSEPR model and have the same geometry as the VSEPR domains.''[109] Moreover, it has been shown that ''there exists a faithful mapping of the electrostatic electron–electron repulsion between the ELF basins and the Gillespie–Nyholm rules of the VSEPR model''.[153]

There is a formal analogy between the VSEPR model and the first theorem of Hohenberg and Kohn.[46] This theorem establishes that the external potential, *i.e.* the nucleus–nucleus and electron-nuclei coulombic potential, of an *N* electron system in the ground state is a unique functional of the one electron density and conversely. As the external potential fixes the hamiltonian, it determines the *N*-electron wave function and, therefore, the pair densities. This means that for a given ground state electron density there is one and only one set of nuclear coordinates and alternatively for a given set of nuclear coordinates there is one and only one ground state electron density. In the VSEPR model the equilibrium molecular geometry, in other words the external potential, is determined by the arrangement of the electronic domains of the central atom valence shells which is a property of the electron density. A reciprocal formulation of the VSEPR rules would provide the electronic domain arrangements expected from any given geometry. For a given geometry, the number of electronic domains and their possible arrangements depend upon the number of electrons in the valence shell of the central atom, the number of ligands, their electronegativity and possible conjugation effects. Table 1 provides the possible geometries and arrangements of electronic domains for local nuclear configurations involving at most three ligands around a given center and their compliance with the VSEPR arrangement. Except for few exceptions belonging to inorganic chemistry and documented in the literature,[154–156] the equilibrium geometries always comply the VSEPR rules. For deformations which qualitatively change the geometry around the central atom, *i.e.* linear to V-shape, triangular to trigonal pyramid, triangular pyramid to triangular, the compliance with the VSEPR arrangement can be achieved by the reorganization of the electronic domains of the valence shell of the central atom. This is possible if the bonding domains at the equilibrium geometry are enough electron rich to enable the necessary density transfers, in practice at least one of the bond from the central atom A is a multiple bond (Y = A–X, Y = A–X, Y = AX_2). The compliance with VSEPR implies the creation of a new non-bonding domain on top of the central atom, the system therefore evolves from a SSD to another and a density transfer from the most electron rich bonding domain toward this new domain is initiated. This situation will be referred to as VSEPR compliant. The non-compliance with VSEPR usually corresponds to cases in which the bonds around the central atom are single bonds, *i.e.* AX_2, AX_3. During the bending of AX_2 or the pyramidalization of AX_3, the system remains in the same SSD and no noticeable density transfer is expected. In this case the non equilibrium arrangements will be said VSEPR defective because compliance requires an additional domain in the valence shell of A. A triangular pyramid structure corresponds to an arrangement involving three bonding and one non-bonding domains which distort in a non-equilibrium planar triangular structure with two non-bonding domains on each sides of the local symmetry plane. The electron population of these latter is about the half of that of the single non bonding domain of the equilibrium structure and the standard VSEPR rules no more apply because

Table 1 Possible electronic domain arrangements and substituent geometries around a central atom bonded to 2 and 3 ligands

Electronic domains			
Bonding	Non-bonding	Geometry	VSEPR compliance
2	0	Linear	VSEPR compliant
2	0	V-shape	VSEPR defective
2	1	V-shape	VSEPR compliant
2	2	V-shape	VSEPR compliant
2	3	Linear	VSEPR compliant
3	0	Triangular	VSEPR compliant
3	0	Trigonal pyramid	VSEPR defective
3	1	Trigonal pyramid	VSEPR compliant
3	2	T-shape	VSEPR compliant
3	2	Triangular	Pseudo VSEPR

the repulsion between bonding domains is larger than that between the half-filled non bonding domains. The preferred arrangement is a trigonal bipyramid with the ligands in equatorial position. Such an arrangement will be called pseudo-VSEPR because it correspond to the interchange of the bonding and non-bonding domain positions. This occurs, for example in the inversion of ammonia[78] and in the back side attack SE_2 electrophilic substitution mechanism where the bonding and non-bonding domains are respectively in equatorial and apical positions.

6 Application to chemical reactivity and reaction mechanisms

6.1 Reactivity of VSEPR defective arrangements

In the context outlined in the previous section, the VSEPR ideas can be used to characterize and understand some aspects of the chemical reactivity. Compliance with VSEPR is expected to stabilize non equilibrium structures whereas defective VSEPR arrangements have an inherent instability which explains their reactivity. The compliance with VSEPR can be achieved by the formation of a dative bond with another reactant having a non-bonding domain available. The principal origin of a VSEPR defective arrangement is an effective number of pairs less than four in the valence shell of the central atom which is either due to the group of the central atom or to strong electron withdrawing effects of its substituents. The Lewis acidity of the halides of the elements belonging to groups II and XIII, the addition on carbonyl groups and the nucleophilic aromatic substitutions are examples of the reactivity of such structures.

The halides of the elements of groups II and XIII have formally two and three electron pairs in the valence shell of the central atom They spontaneously bind to Lewis bases such NH_3. The addition reactions of ammonia on $BeCl_2$ and BF_3 are both exothermic by 120 kJ $mole^{-1}$ and 129 kJ $mole^{-1}$,[157] respectively. The electrophilicity index,[158] ω, of these two molecules increases with the deformation. The minimum of the ground state of the Born–Oppenheimer energy surface of $BeCl_2$ is linear but the vibrationally averaged structure is bent with $\angle$ ClBeCl = 163°.[159] The frequency of the π_u bending mode responsible for the bent structure is low, 252 cm^{-1},[159] which explains the absence of barrier in the addition reaction. The electrophilicity of the vibrationally averaged bent structure is larger than that of the linear one by about 0.2 eV. For a bent angle of 120° the increase of ω reaches 1.4 eV. The same description holds for the boron trifluoride for which the active bending vibrational mode, ν_2, is observed at 691 cm^{-1}.[160] The increase of the electrophilicity upon pyramidalization is calculated to be as large as 1.9 eV for $\angle$ FBF = 109.47°.

There are formally four electron pairs in the valence shell of the carbon of a carbonyl group and, so, the out of plane deformation is expected to induce the transfer of a pair from the C═O double bond towards the carbon in order to satisfy the VSEPR stability requirement. However, the large electronegativity of the oxygen polarizes the CO bond and the VSEPR defective arrangement happens to be favoured in the off-equilibrium non planar geometry, *i.e.*:

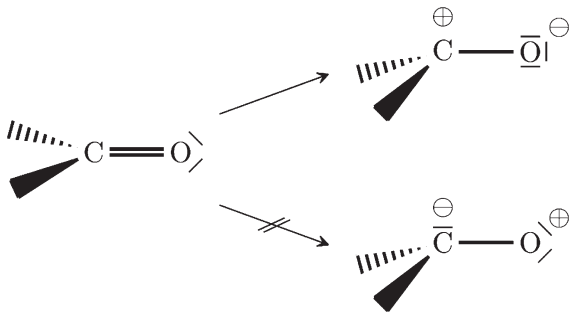

The carbonyl addition usually starts by the attack of the carbon centre by a nucleophilic reagent when it is catalysed by a base and by the protonation of the oxygen atom when catalysed by an acid. However, the pyramidalization of the carbonyl group is not accompanied of a noticeable variation of the electrophilicity index.

The out of plane bending of a substituent is the driving internal coordinate of the aromatic substitution. As the aromatic ring is electron rich, the standard VSEPR compliant scheme is favoured enabling a Lewis acid to form a dative bond in the Wheland complex. If the aromatic ring is already substituted by electron withdrawing groups, the VSEPR defective structure could be favoured enabling a nucleophilic substitution.

For most organic reactions, the number of ligands around a reactive centre hardly ever exceeds four. The only active deformations for which the number of non bonding electronic domains varies are the bending of colinear bonds, the out-of-plane bending and the ligand bending which locally brings the system in a planar geometry. Each of these motions will be illustrated by textbook organic reactions and the predictions of the method compared to the results of quantum chemical studies in which the ELF basin populations along a reaction pathway have been computed.

6.2 Bending of colinear bonds

The bending of colinear bonds is the simplest deformation enabling the creation of a new non bonding domain in order to ensure the VSEPR compliance. This implies a density transfer from a multiple bond toward the new non-bonding domain on top of the central atom, *i.e.*:

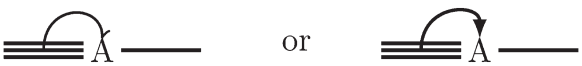

according to the amount of transferred density. This motion gives rise to a very strong vibrational band observed below 1000 cm^{-1} and therefore the creation of the new atomic domains requires a relatively small amount of energy.

The Bergman's cyclization of (*Z*)-hexa-1,5-diyne-3-ene[161] is a typical example involving the bending of colinear bonds which has been theoretically investigated by the BET technique.[125] The product, *p*-benzyne, is described as a singlet biradical and

therefore two non-bonding domains with population of *ca.* 1 e^- of integrated spinless density are expected on two carbon in *para* position. In order to achieve the cyclization one has first to bend the C(3)–C(2)≡C(1) and C(4)–C(5)≡C(6) groups. The corresponding A_1 normal modes are calculated at 448 and 640 cm^{-1}. The fulfillment of the VSEPR rules implies the creation of non-bonding domains on top of C(2) and C(5) associated with charge transfers of 1 e^- from each triple bond. This deformation bringing the terminal hydrogen atoms close together induces the bending of the C≡C–H groups associated with electron density transfer from the former triple bonds toward non-bonding domains on top of carbons C(1) and C(6) which ultimately merge into a single bond C(1)–C(6). There is finally a delocalization of the C–C bonds which stabilizes the *p*-benzyne. The mechanism is represented in the scheme below.

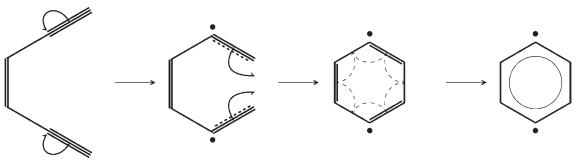

The dashed curved fish-hook arrows represent density transfers of 0.5 e^- which occur during the aromatization process. This picture is confirmed by the sequence of the catastrophes reported in the BET study[125] and by the evolution of the basin populations displayed in Fig. 3.

In the trimerization of acetylene reaction, the symmetric bending of the three acetylene molecules is responsible for an electron density transfer from the triple bonds to non bonding domains on each carbons which further merge to yield the benzene molecule. The BET analysis[141] finds six simultaneous fold catastrophes corresponding to the creation of non bonding domains on the carbon atoms due to the symmetric bending of the three acetylene fragments followed by three cusp catastrophes accounting for the formation of three C–C bonds.

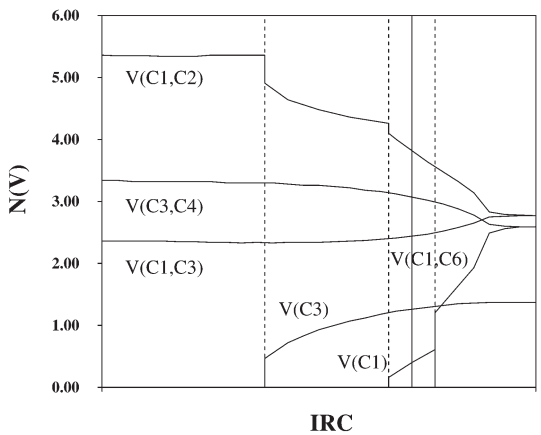

Fig. 3 ELF valence basin populations along the IRC path for the Bergman reaction. Multiple bond populations have been condensed. The vertical lines materialize the structural stability domains boundaries. Atom are numbered according to IUPAC conventions.

The angular deformations necessary to link the reactants to the products of the 1,3 dipolar cycloaddition of acetylene and fulminic acid molecules are the bending modes δ_{NCH}, δ_{CNO} of the fulminic acid and the anti-symmetric bending of acetylene, observed respectively at 224, 537 and 613 cm^{-1}. We assume that the nuclear displacements along the reaction pathway follow the order of ascending frequencies and we will only consider the dominant mesomeric structure, H–C≡$N^{\oplus}$–$O^{\ominus}$, of the fulminic acid as a starting point. The bending of the H–C≡N is expected to yield a VSEPR compliant arrangement, in which the non-bonding domain created on top of the carbon is populated by a density transfer of 1 e^- from the triple bond. A second density transfer of 2 e^- from the triple bond is then associated with the bending of C≡N–O consistent with the nitrogen lone pair of the Lewis structure of 1,2 oxazole. On the acetylene side, the anti-symmetric bending would be normally associated with a density transfer of 1 e^- from the triple bond towards non-bonding domains on both carbons in order to comply with VSEPR. However, the electric field of the $N^{\oplus}$–$O^{\ominus}$ dipole favours a VSEPR defective carbon in front of the oxygen atom. The carbon non-bonding domains merge to form the C–C single bond followed by the formation of a C–O dative bond accompanied by a density transfer of 1 e^- electron from former acetylene triple bond towards the new C–C single bond enabling a delocalization consistent with the aromaticity of 1,2 oxazole. This scenario represented by the pushing arrow scheme:

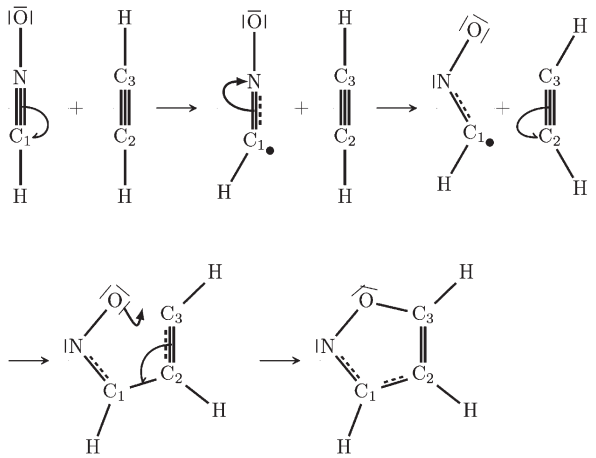

recovers most of the features of the population graph of the BET analysis[140] displayed Fig. 4. The small differences are on the one hand is the behaviour of V(C1) and V(C1,N): at angles close to 180° V(C1) is already present, at the transition state it splits to yield a second non bonding basin, V′(C1) which merges with V(C2) to form the C–C single bond. Once this bond is formed V(C1) merges with V(C1,N). This rather complicated mechanism can be interpreted by invoking a second mesomeric structure of HCNO in which the carbon has a lone pair. On the other hand the weakly populated V(C3) basin can be interpreted as a footprint of the electric field free transfers associated with the anti-symmetric bending of acetylene. It is worth noting that the evolution of the basin populations of the

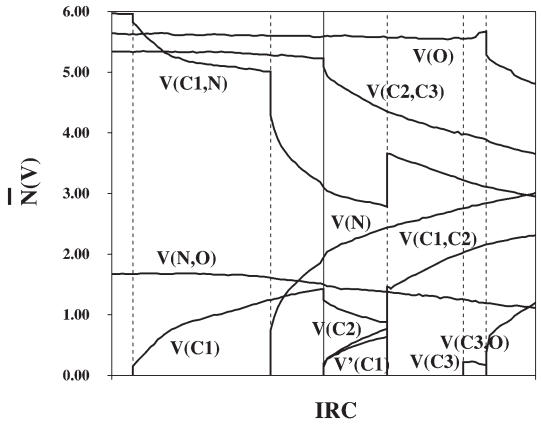

Fig. 4 ELF valence basin populations along the IRC path of the C_2H_2 + HCNO1,3-dipolar cycloaddition reaction. Multiple bond or non-bonding basin populations have been condensed. All vertical lines materialize a structural stability domains transition dashed lines, the full vertical line moreover corresponds to the transition state.

1,3 dipolar cycloaddition of benzonitrile oxide and cyclopentene[145] is very similar to that displayed in Fig. 4.

6.3 Out-of-plane bending

The out-of-plane bending is a deformation which plays an important role in many reactions involving olefines or aromatic molecules. In the infrared spectra, the corresponding normal modes give rise to strong bands below 1000 cm^{-1}. The local pyramidalization implies the creation of a non-bonding domain on the central atom through density transfers from the adjacent bonds (mostly from the double bond) in order to get a compliant VSEPR arrangement, *i.e.*

The density transfer is enhanced when it occurs in front of the electrophilic part of the other reactant as in the Wheland σ-complex formation of the aromatic substitution reaction. In the example of

$$C_6H_6 + Cl_2 \xrightarrow{AlCl_3} C_6H_5Cl + HCl$$

the reaction is catalysed by $AlCl_3$. In a first step, Cl_2 is involved in the π-complex in bridging position between the Lewis acid catalyst and a carbon atom of the benzene ring. The Cl–Cl bond is weakened and strongly polarized with its positive head close to the carbon. The out of plane bending of the hydrogen bonded to this carbon gives rise to a non-bonding domain on top of the carbon implying a density transfer from the two nearest C–C bonds. The process is enhanced by the proximity of the electrophilic centre which enables this latter to bind (in this case C_6H_6 locally behaves like a Lewis base) to form the σ-Wheland complex. Fig. 5 displays the ELF localization domains of π- and σ-complexes of this reaction. The ELF population analysis shows a density transfer of 0.47 *e* from the C_{ipso}–C_{ortho} bonds towards the C–Cl one as well as the enhancement of the C_{meta}–C_{para} bond populations at the expense of that of the C_{ortho}–C_{meta} ones.

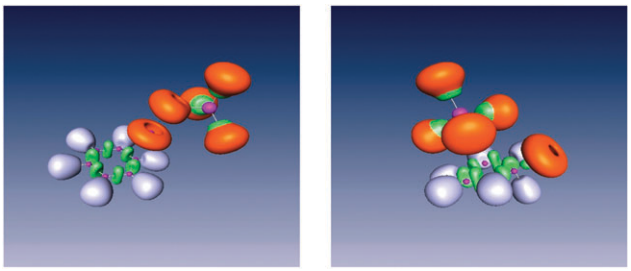

Fig. 5 ELF localization domains of the π-(left) and σ-(right) complexes of the aromatic electrophilic substitution catalysed by $AlCl_3$. Colour code: magenta = core, red = non-bonding, green bonding, light blue = C–H bonds.

The Diels–Alder addition of cyclopropene and 1,3 butadiene implies the pyramidalization of the $=CH_2$ groups of both molecules. These out-of-plane deformations correspond to the normal modes observed at 575 and *ca.* 910 cm^{-1} in cyclopropene and 1,3 butadiene, respectively. The ascending order of frequencies hypothesis suggests that a first density transfer of 1 e^- from the cyclopropene double bond toward the top of the C_1 and C_6 atoms occurs in order to ensure the VSEPR compliance of the electronic domain arrangements around these two latter atoms. The VSEPR compliance of the terminal carbons, C_2 and C_5, implies density transfers of 1 e^-, from the 1,3 butadiene double bonds toward these atoms. Finally, an amount of 2 e^-, is transferred from these latter bonds toward the C_3, C_4. The electron pushing scheme:

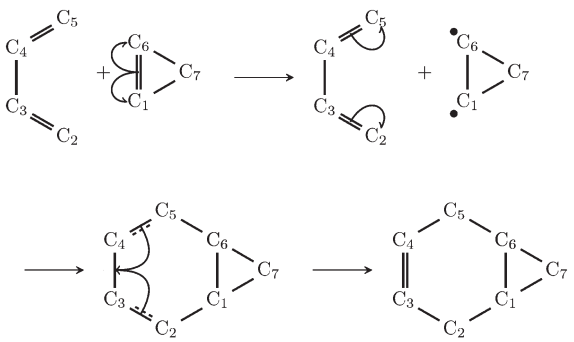

is in very good agreement with the BET population evolution graph displayed Fig. 6.

6.4 Pyramidal to planar deformation

This type of deformation is encountered in aliphatic substitutions it may follows the breaking of a bond in tetracoordinated tetrahedral site. Rather than the determination of the density transfers which are rather straightforward, the compliance of the VSEPR rules provides a chemical explanation of the stereochemical aspects of SN_2 and SE_2 reaction mechanism. In the aliphatic nucleophilic substitution, two mechanisms can be invoked. On the one hand is the back side attack of the nucleophilic group which yields an inversion of configuration

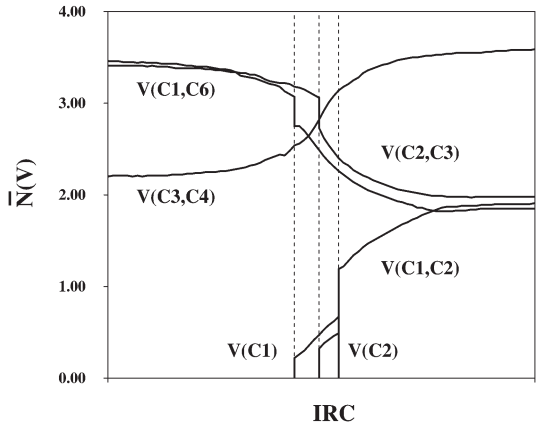

Fig. 6 ELF valence basin populations along the IRC path of the C_3H_4 + C_4H_6 Diels Alder addition reaction. Multiple bond or non-bonding basin populations have been condensed. Atom are numbered according to IUPAC conventions for bicyclo [4.1.0] hept-3-ene. Vertical lines materialize a structural stability domains transition dashed lines.

and on the other hand the front side attack, the result of which is the retention of configuration.

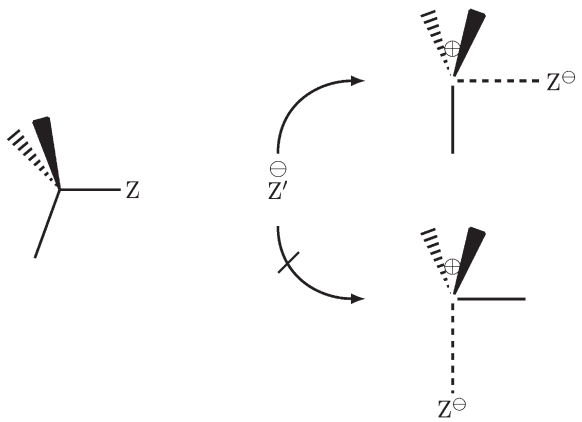

The back side attack implies the formation of a planar triangular carbocation in which the arrangement of the electronic domains is consistent with the VSEPR rules. The front side attack yields a triangular pyramidal VSEPR defective carbocation. Therefore, the backside attack channel is energetically favoured, the calculated barriers being calculated to be lower by about 200 kJ mole^{-1} than for the front side attack.[162] In the reaction

$$Cl^- + H_3CBr \rightarrow ClCH_3 + Br^-$$

the symmetric bending $\delta_s(CH_3)$ is the driving mode which accounts for the deformation of the methyl group. In the transition state CH_3 is planar and positively charged because the opening of the methyl group has yielded a transfer of the C–Br bond density towards the bromine lone pairs. This transfer is assisted by the backside approach the chlorine anion and the IRC indicates that the formation of the C–Cl bond is simultaneous with the breaking of the C–Br bond. This mechanism is consistent with the result of a recent study of the SN_2 mechanism by Joubert *et al.*[163] and of the BET analysis.[148] The ELF localization domains represented in Fig. 7 for different steps of

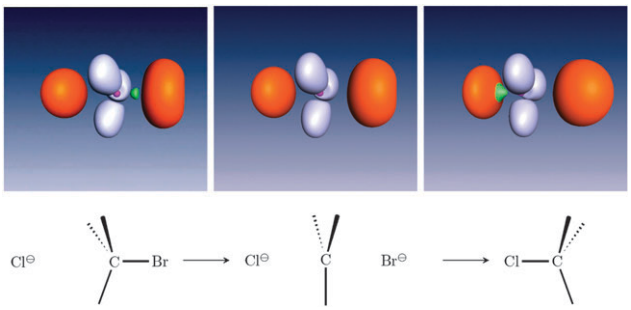

Fig. 7 Evolution of the ELF localization domains along the reaction path of the Cl^- + H_3CBr → $ClCH_3$ + Br^- nucleophilic substitution. Color code: magenta = core, red = non-bonding, light blue = C–H bonds.

the reaction clearly evidence the mechanism if this typical Ingold's SN_2 reaction. In the alternative SN_1 reaction, the substituents of the reactive centre sterically hamper the approach of the nucleophilic reagent and therefore, the transition state is a VSEPR consistent planar CR_3^+ cation.

In the aliphatic electrophilic substitution, the front side attack yields a triangular pyramidal arrangement of the CR_3^- carbanion which is the VSEPR compliant structure. The trigonal bipyramid arrangement of the electronic domains expected for the backside attack is a pseudo VSEPR arrangement where each non bonding domain has a population of one electron. This structure corresponds to the top of the inversion barrier.

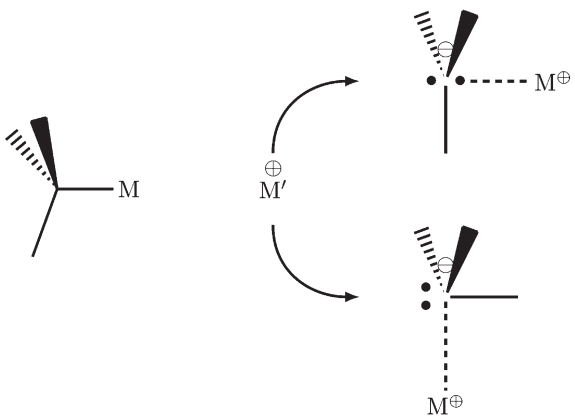

Indeed, the transition states corresponding to the two attacks are often close in energy. In the lithium cation exchange reaction:

$$LiCH_3 + Li^+ \rightarrow Li^+ + CH_3Li$$

the energy of the backside attack transition state is calculated to be lower by 14 kJ mol^{-1} that the front side attack one. Fig. 8 displays the localization domains for the two transition state geometries. In both transition state structures the CH_3^- moiety forms a specific chemical entity and the bonding with the Li^+ centres belongs to the ionic type. However, in the front side attack case the structure of the transition state is consistent with the three-centre two-electron (3c–2e) proposed for the bromination of alkanes.[164]

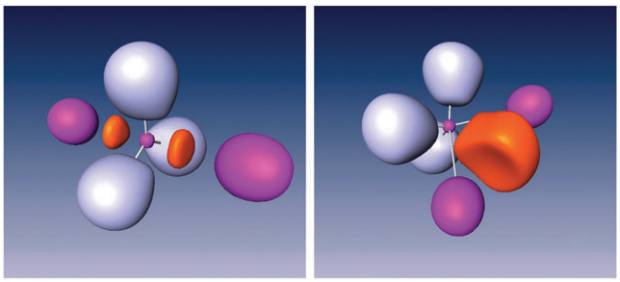

Fig. 8 ELF = 0.85 localization domains of the transition states of the $LiCH_3 + Li^+ \rightarrow Li^+ + CH_3Li$ substitution for the back side (left) and front side (right) attacks. Colour code: magenta = core, red = non-bonding, light blue = C–H bonds.

7 Conclusions and perspectives

The approach presented here is a contribution to the understanding of electron density transfers in terms of the evolution of the nuclear geometry along the reaction pathway linking reactants to product. One of the advantages of casting theories of chemical reactivity in terms of $\rho(\mathbf{r})$ is that this local function is defined within the exact many body theory as a quantum observable which is also an experimentally accessible scalar field. The partition of the electron density domains into electronic domains minimizing the variance of their populations as achieved by ELF enables a sound description of the bonding which matches the Lewis representation. The evolution of these domains along the reaction pathway is used to characterize a reaction mechanism. The examples presented here illustrate the potential ability of the method to describe complex mechanisms and show how theoretical and computational chemistry can directly establish reaction mechanisms in intuitive terms and unprecedented details. The BET method enables to search for the degree of fitness of the Lewis hypothesis of chemical bonding as an electron pairing phenomena. On this basis we should be able to quantitatively predict the reaction mechanics and outcome of the physical processes that lead from reactants to products *via* the corresponding transition structure and possible intermediates.

The chemical explanation of the results of the BET method rely on two simple ideas. The first is to consider the electronic domains of the VSEPR model rather than the Lewis's electron pairs as the chemical objects subjected to the density transfers. The arrangements of the electronic domains of the reactants and products equilibrium geometry satisfy the VSEPR rules. Along the reaction pathway the rearrangement of the electronic domains is driven by the deformations of the geometry of the nuclei and by the population of the valence shell of the central atom. The second idea is that these deformations have their origin in the vibrational modes which follow the IRC because the vibrational energy is the main contribution of the activation energy of thermally controlled chemical reaction. The Rice and Teller's principle of least motion[165] and the Hammond's postulate[166] can be used to guess a realistic reaction pathway. The qualitative predictions made with this approach can be validated by the BET analysis which provides a one to one correspondence between the structural stability domains and the sequence of arrangements. For all reactions studied in the BET framework up to now, this model nicely works. Moreover, the force constants of the considered vibrational modes provide information on the sequences of rearrangements.

The potential applications of the method cover the determination of the mechanisms of reactions belonging to organic as well as inorganic chemistry as done in recent studies.[79,81,82,122,136,143,146,167–173] We believe that the approach proposed here can thus be useful not only in a variety of circumstances to provide quantitative insights into the nature of chemical reactivity and for the modelling of reaction mechanism, based on the electron density transfers but also it should become a powerful tool in the chemical education of undergraduate students because our theoretical findings can serve as a general guideline for the study and analysis of the chemical structure and reaction mechanisms.

Our understanding of the chemical structure and reactivity is usually built up from and dependent upon such intuitive concepts as atom in molecule, chemical bond, lone pair, Lewis structure, *etc.* In particular, a common way to rationalize and predict chemical reactivity from the density viewpoint is to use electron pushing arrows, and then the reaction mechanisms in chemistry are often indicated by curly arrows in Lewis structures. This prototypical representation is provided by electron pushing formalisms where electron flow is represented with curly arrows, and it is a powerful tool for the prediction of chemical reactions. The curly arrows intend to represent the net change of electron density from one molecular structure to the other, but they can not represent the chemical reaction. Electron density transfer processes do not take place between atoms and chemical bonds as chemical reactions occurs. That is, they do not represent how the electrons really move, and thus they do not represent the reaction mechanism. In other words, while these curly arrows account for changes in the electronic structure from reactant to product, they do not give an entirely appropriate picture of electron rearrangement based on physical grounds. This situation might be improved, and in this communication we propose an alternative view of electron flows of molecules when undergoing chemical reactions from the perspective of BET analysis and this is capable to provide qualitative and quantitative information for characterizing reaction mechanism. Our hope is to recover the electron pushing formalisms, *i.e.* curly arrows and that the concepts and examples described can be capable to provide qualitative and quantitative information for characterizing reaction mechanism.

Acknowledgements

We wish to thank Professors R. J. Gillespie, Henry H. Rzepa and Patrick Chaquin and L. R. Domingo for stimulating discussions and the referees for their very constructive comments.

References

1 C. K. Ingold, *J. Chem. Soc.*, 1933, **143**, 1120–1127.
2 C. K. Ingold, *Chem. Rev.*, 1934, **15**, 225–274.
3 J. H. Ridd, *Chem. World*, 2008, **5**, 50–53.

4 D. O'Hagan and D. Lloyd, *Chem. World*, 2010, **7**, 54–57.
5 G. N. Lewis, *J. Am. Chem. Soc.*, 1916, **38**, 762–786.
6 I. Langmuir, *J. Am. Chem. Soc.*, 1919, **41**, 868–934.
7 I. Langmuir, *J. Am. Chem. Soc.*, 1919, **41**, 1543–1559.
8 I. Langmuir, *J. Am. Chem. Soc.*, 1920, **42**, 274–292.
9 J. J. Thomson, *Philos. Mag.*, 1921, **41**, 510–544.
10 J. A. N. Friend, *J. Chem. Soc., Trans.*, 1921, **119**, 1040–1047.
11 A. Lapworth, *J. Chem. Soc., Trans.*, 1922, **121**, 416–427.
12 W. O. Kermack and R. Robinson, *J. Chem. Soc., Trans.*, 1922, **121**, 427–440.
13 H. Budzikiewicz, C. Djerassi and D. H. Williams, *Interpretation of Mass Spectra of Organic Compounds*, Holden-Day, San Francisco, 1965.
14 S. Alvarez, *Angew. Chem., Int. Ed.*, 2012, **51**, 590–600.
15 D. A. Evans, *Angew. Chem., Int. Ed.*, 2014, **53**, 11140–11145.
16 R. F. Hunter, *The electronic theory of chemistry; an introductory account*, Longmans, Green & Co, New York, 1934.
17 C. K. Ingold, *Structure and Mechanisms in Organic Chemistry*, Bell and Sons, London, 1953.
18 E. S. Gould, *Mechanism and structure in organic chemistry*, Holt, 1959.
19 P. Sykes, *A Guidebook to Mechanism in Organic Chemistry*, Wiley, New York, 1962.
20 D. E. Levy, *Arrow-Pushing in Organic Chemistry: An Easy Approach to Understanding Reaction Mechanisms*, John Wiley & Sons, Inc., 2008.
21 W. Salmon, *Explanation and the causal structure of the world*, Princeton University Press, Princeton, NJ, 1984.
22 V. Gineityte, *Int. J. Quantum. Chem.*, 2003, **94**, 302–316.
23 V. Gineityte, *Z. Naturforsch.*, 2009, **64a**, 132–148.
24 V. Gineityte, *Lith. J. Phys.*, 2011, **51**, 107–126.
25 T. Okuyama and H. Maskill, *Organic Chemistry. A mechanistic approach*, Oxford University Press, 2013.
26 H. S. Rzepa, *A curly-arrow pushing manual*, http://www.ch.imperial.ac.uk/rzepa/blog/?p = 11741.
27 J. F. Gonthier, S. N. Steinmann, M. D. Wodrich and C. Corminboeuf, *Chem. Soc. Rev.*, 2012, **41**, 4671–4687.
28 K. Fukui, T. Yonezawa and H. Shinghu, *J. Chem. Phys.*, 1952, **20**, 722.
29 R. B. Woodward and R. Hoffmann, *Angew. Chem., Int. Ed. Engl.*, 1969, **8**, 781–932.
30 L. Pauling, *J. Am. Chem. Soc.*, 1931, **53**, 1367–1400.
31 L. Pauling, *J. Am. Chem. Soc.*, 1931, **53**, 3225–3237.
32 L. Pauling, *J. Am. Chem. Soc.*, 1932, **54**, 988–1003.
33 L. Pauling, *The Nature of the Chemical Bond*, Cornell University Press, Ithaca, 1948.
34 S. S. Shaik and A. Shurki, *Angew. Chem., Int. Ed.*, 1999, **38**, 586–625.
35 A. Shurki, E. Derat, A. Barrozo and S. C. L. Kamerlin, *Chem. Soc. Rev.*, 2015, **44**, 1037–1052.
36 G. N. Lewis, *J. Chem. Phys.*, 1933, **1**, 17–28.
37 R. G. Parr, R. A. Donnelly, M. Levy and W. E. Palke, *J. Chem. Phys.*, 1978, **68**, 3801–3807.
38 R. G. Parr and R. G. Pearson, *J. Am. Chem. Soc.*, 1983, **105**, 7512–7516.
39 P. Geerlings, F. De Proft and W. Langenaeker, *Chem. Rev.*, 2003, **103**, 1793–1873.
40 S. S. Shaik, *J. Am. Chem. Soc.*, 1981, **103**, 3692–3701.
41 G. Leroy, M. Sana, L. A. Burke and M. T. Nguyen, in *Theory of Chemical Reactions*, ed. R. Daudel, S. Diner and J. P. Malrieu, Reidel, Dordrecht, 1979, pp. 395–448.
42 G. Knizia and J. E. M. N. Klein, *Angew. Chem., Int. Ed.*, 2015, **54**, 5518–5522.
43 P. B. Karadakov, D. L. Cooper and J. Gerratt, *Theor. Chem. Acc.*, 1998, **100**, 222–229.
44 R. D. Harcourt and A. Schulz, *J. Phys. Chem. A*, 2000, **104**, 6510–6516.
45 P. Balanarayan, R. Kavathekar and S. R. Gadre, *J. Phys. Chem. A*, 2007, **111**, 2733–2738.
46 P. Hohenberg and W. Kohn, *Phys. Rev.*, 1964, **136**, B864–B871.
47 D. Stalke, *Chem. – Eur. J.*, 2011, **17**, 9264–9278.
48 D. Chopra, *J. Phys. Chem. A*, 2012, **116**, 9791–9801.
49 P. L. A. Popelier, in *Structure and Bonding. Intermolecular Forces and Clusters*, ed. D. J. Wales, Springer, Heidelberg, 2005, vol. 115, pp. 1–56.
50 P. L. A. Popelier and E. A. G. Brémond, *Int. J. Quantum. Chem.*, 2009, **109**, 2542–2553.
51 S. Noury, X. Krokidis, F. Fuster and B. Silvi, *Comput. Chem.*, 1999, **23**, 597–604.
52 P. L. A. Popelier, *Comput. Phys. Commun.*, 1996, **93**, 212–240.
53 M. Kohout, *Chemical Bonding Analysis in Direct Space*, http://www.cpfs.mpg.de/ELF, 2002.
54 F. Biegler-König, J. Schönbohm and D. Bayles, *J. Comput. Chem.*, 2001, **22**, 545–559.
55 A. Otero de la Roza, M. Blanco, A. Martín Pendás and V. Luaña, *Comput. Phys. Commun.*, 2009, **180**, 157–166.
56 R. F. W. Bader, *Atoms in Molecules: A Quantum Theory*, Oxford Univ. Press, Oxford, 1990.
57 R. J. Gillespie and P. L. A. Popelier, *Chemical Bonding and Molecular Geometry*, Oxford University Press, Oxford, 2001.
58 B. Silvi and A. Savin, *Nature*, 1994, **371**, 683–686.
59 B. de Courcy, L. G. Pedersen, O. Parisel, N. Gresh, B. Silvi, J. Pilmé and J.-P. Piquemal, *J. Chem. Theory Comput.*, 2010, **6**, 1048–1063.
60 J. Pilme, H. Berthoumieux, V. Robert and P. Fleurat-Lessard, *Chem. – Eur. J.*, 2007, **13**, 5388–5393.
61 A. de la Lande, J. Maddaluno, O. Parisel, T. A. Darden and J. P. Piquemal, *Interdiscip. Sci.: Comput. Life Sci.*, 2010, **2**, 3–11.
62 S. Berski, J. Andrés, B. Silvi and L. R. Domingo, *J. Phys. Chem. A*, 2006, **110**, 13939–13947.
63 J. Poater, M. Duran, M. Solà and B. Silvi, *Chem. Rev.*, 2005, **105**, 3911–3947.
64 F. Pauzat, J. Pilmé, J. Toulouse and Y. Ellinger, *J. Chem. Phys.*, 2010, **133**.
65 P. Rivera-Fuentes, J. L. Alonso-Gómez, A. Petrovic, P. Seiler, F. Santoro, N. Harada, N. Berova, H. Rzepa and F. Diederich, *Chem. – Eur. J.*, 2010, **16**, 9796–9807.
66 D. Kozlowski and J. Pilmé, *J. Comput. Chem.*, 2011, **32**, 3207–3217.
67 S. Jenkins, *Int. J. Quantum Chem.*, 2013, **113**, 1603–1608.
68 T. S. Koritsanszky and P. Coppens, *Chem. Rev.*, 2001, **101**, 1583–1628.
69 P. Coppens, *X-ray charge densities and chemical bonding*, Oxford Univ. Press, Oxford, 1997.
70 P. L. A. Popelier, *Atoms In Molecules: an Introduction*, Pearson Education Group, Harlow, 2000.
71 V. G. Tsirelson and R. P. Ozerov, *Electron density and bonding in crystals*, Institute of physics publishing, Bristol, 1996.
72 G. A. Jeffrey and W. Saenger, *Hydrogen Bonding in Biological Structures*, Springer Verlag, Berlin, 1991.
73 C. Matta and R. J. Boyd, *The Quantum Theory of Atoms in Molecules*, From Solid State to Drug Design, Wiley-VCH, Weinheim2007.
74 *Modern Charge-Density Analysis*, ed. C. Gatti and P. Macchi, Springer Netherlands, Dordrecht, 2012.
75 Y. Tal, R. F. W. Bader, T. T. Nguyen-Dang, M. Ojha and S. G. Anderson, *J. Chem. Phys.*, 1981, **74**, 5162–5167.
76 A. Morgenstern, C. Morgenstern, J. Miorelli, T. Wilson and M. E. Eberhart, *Phys. Chem. Chem. Phys.*, 2016, **18**, 5638–5646.
77 N. O. J. Malcolm and P. L. A. Popelier, *J. Phys. Chem. A*, 2001, **105**, 7638–7645.
78 X. Krokidis, S. Noury and B. Silvi, *J. Phys. Chem. A*, 1997, **101**, 7277–7282.
79 P. González-Navarrete, J. Andrés and S. Berski, *J. Phys. Chem. Lett.*, 2012, **3**, 2500–2505.
80 N. Gillet, R. Chaudret, J. Contreras-García, W. Yang, B. Silvi and J.-P. Piquemal, *J. Chem. Theory Comput.*, 2012, **8**, 3993–3997.
81 J. Andrés, P. González-Navarrete and V. S. Safont, *Int. J. Quantum. Chem.*, 2014, **114**, 1239–1252.
82 J. Andrés, L. Gracia, P. González-Navarrete and V. S. Safont, *Comput. Theor. Chem.*, 2015, **1053**, 17–30.
83 V. S. Safont, P. Gonzalez-Navarrete, M. Oliva and J. Andres, *Phys. Chem. Chem. Phys.*, 2015, **17**, 32358–32374.
84 R. J. Gillespie and R. S. Nyholm, *Q. Rev., Chem. Soc.*, 1957, **11**, 339–380.
85 R. J. Gillespie, *Molecular Geometry*, Van Nostrand Reinhold, London, 1972.
86 R. J. Gillespie and E. A. Robinson, *Angew. Chem., Int. Ed. Engl.*, 1996, **35**, 495–514.
87 R. Daudel, *Compt. Rend. Acad. Sci.*, 1953, **237**, 601–603.
88 R. Daudel, S. Odiot and H. Brion, *J. Chim. Phys. Phys.-Chim. Biol.*, 1954, **51**, 74–77.
89 R. Daudel, H. Brion and S. Odiot, *J. Chem. Phys.*, 1955, **23**, 2080–2083.
90 E. Cancès, R. Keriven, F. Lodier and A. Savin, *Theor. Chem. Acc.*, 2004, **111**, 373–380.
91 A. Gallegos, R. Carbó-Dorca, F. Lodier, E. Cancès and A. Savin, *J. Comput. Chem.*, 2005, **26**, 455–460.
92 A. Scemama, M. Caffarel and A. Savin, *J. Comput. Chem.*, 2007, **28**, 442.

93 O. M. Lopes, B. Braïda, M. Causà and A. Savin, in *Advances in the Theory of Quantum Systems in Chemistry and Physics*, ed. E. P. Hoggan, J. E. Brändas, J. Maruani, P. Piecuch and G. Delgado-Barrio, Springer Netherlands, Dordrecht, 2012, ch. Understanding Maximum Probability Domains with Simple Models, pp. 173–184.
94 E. Francisco, A. Martín Pendás and M. A. Blanco, *J. Chem. Phys.*, 2007, **126**, 094102.
95 A. Martín Pendás, E. Francisco and M. A. Blanco, *J. Chem. Phys.*, 2007, **127**, 144103.
96 A. Martín Pendás, E. Francisco and M. A. Blanco, *J. Phys. Chem. A*, 2007, **111**, 1084–1090.
97 A. Martín Pendas, E. Francisco and M. A. Blanco, *Phys. Chem. Chem. Phys.*, 2007, **9**, 1087–1092.
98 E. Francisco, A. Martín Pendás and M. Blanco, *Comput. Phys. Commun.*, 2008, **178**, 621–634.
99 E. Francisco, A. Martín Pendás and M. Blanco, *J. Chem. Phys.*, 2009, **131**.
100 M. Causà and A. Savin, *J. Phys. Chem. A*, 2011, **115**, 13139–13148.
101 S. Diner and P. Claverie, in *Localization and Delocalization in Quantum Chemistry*, ed. O. Chalvet, R. Daudel, S. Diner and J. P. Malrieu, Reidel, Dordrecht, 1976, vol. II, pp. 395–448.
102 B. Silvi, *Phys. Chem. Chem. Phys.*, 2004, **6**, 256–260.
103 B. Silvi, I. Fourré and E. Alikhani, *Monatsh. Chem.*, 2005, **136**, 855–879.
104 P. W. Ayers, *J. Chem. Sci.*, 2005, **117**, 441–454.
105 A. D. Becke and K. E. Edgecombe, *J. Chem. Phys.*, 1990, **92**, 5397–5403.
106 B. Silvi, in *The Chemical Bond – 100 years old and getting stronger.*, ed. P. D. M. Mingos, Springer Berlin Heidelberg, Berlin, Heidelberg, 2016, ch. The Relevance of the ELF Topological Approach to the Lewis, Kossel, and Langmuir Bond Model, pp. 1–35.
107 M. Menéndez, A. Martín Pendás, B. Braïda and A. Savin, *Comput. Theor. Chem.*, 2015, **1053**, 142–149.
108 R. H. Abraham and C. D. Shaw, *Dynamics: The Geometry of Behavior*, Addison Wesley, Redwood City, CA, 1992.
109 R. J. Gillespie and E. A. Robinson, *J. Comput. Chem.*, 2007, **28**, 87–97.
110 B. Silvi, *J. Mol. Struct.*, 2002, **614**, 3–10.
111 A. Tachibana and K. Fukui, *Theor. Chim. Acta*, 1979, **51**, 189–206.
112 A. Tachibana and K. Fukui, *Theor. Chim. Acta*, 1979, **51**, 275–296.
113 K. Fukui, *Acc. Chem. Res.*, 1981, **12**, 363–368.
114 C. Gonzalez and H. B. Schlegel, *J. Chem. Phys.*, 1989, **90**, 2154–2161.
115 C. Gonzalez and H. B. Schlegel, *J. Phys. Chem.*, 1990, **94**, 5523.
116 R. Thom, *Stabilité Structurelle et Morphogénèse*, Intereditions, Paris, 1972.
117 X. Krokidis, V. Goncalves, A. Savin and B. Silvi, *J. Phys. Chem. A*, 1998, **102**, 5065–5073.
118 X. Krokidis, R. Vuilleumier, D. Borgis and B. Silvi, *Mol. Phys.*, 1999, **96**, 265–273.
119 M. E. Alikhani and B. Silvi, *J. Mol. Struct.*, 2004, **706**, 3–6.
120 X. Krokidis, B. Silvi, C. Dezarnaud-Dandine and A. Sevin, *New J. Chem.*, 1998, **22**, 1341–1350.
121 S. Berski and Z. Latajka, *Chem. Phys. Lett.*, 2006, **426**, 273–279.
122 P. González-Navarrete, F. R. Sensato, J. Andrés and E. Longo, *J. Phys. Chem. A*, 2014, **118**, 6092–6103.
123 X. Krokidis, B. Silvi and M. E. Alikhani, *Chem. Phys. Lett.*, 1998, **292**, 35–45.
124 E. Chamorro, J. C. Santos, B. Gómez, R. Contreras and P. Fuentealba, *J. Chem. Phys.*, 2001, **114**, 23–34.
125 J. C. Santos, J. Andrés, A. Aizman, P. Fuentealba and V. Polo, *J. Phys. Chem. A*, 2005, **109**, 3687–3693.
126 V. Polo and J. Andrés, *J. Comput. Chem.*, 2005, **26**, 1427–1437.
127 V. Polo and J. Andres, *J. Chem. Theory Comput.*, 2007, **3**, 816–823.
128 J. Andrés, S. Berski, L. R. Domingo and P. González-Navarrete, *J. Comput. Chem.*, 2012, **33**, 748–756.
129 A. Morales-Bayuelo, *Int. J. Quantum. Chem.*, 2013, **113**, 1534–1543.
130 M. C. Michelini, E. Sicilia, N. Russo, M. E. Alikhani and B. Silvi, *J. Phys. Chem. A*, 2003, **107**, 4862–4868.
131 S. Chiodo, O. Kondakova, M. del Carmen Michelini, N. Russo and E. Sicilia, *Inorg. Chem.*, 2003, **42**, 8773–8782.
132 S. Chiodo, O. Kondakova, M. del Carmen Michelini, N. Russo, E. Sicilia, A. Irigoras and J. M. Ugalde, *J. Phys. Chem. A*, 2004, **108**, 1069–1081.
133 M. del Carmen Michelini, N. Russo and E. Sicilia, *Inorg. Chem.*, 2004, **43**, 4944–4952.
134 M. C. Michelini, N. Russo, M. E. Alikhani and B. Silvi, *J. Comput. Chem.*, 2004, **25**, 1647–1655.
135 M. C. Michelini, N. Russo, M. E. Alikhani and B. Silvi, *J. Comput. Chem.*, 2005, **26**, 1284–1293.
136 S. Berski, F. R. Sensato, V. Polo, J. Andrés and V. S. Safont, *J. Phys. Chem. A*, 2011, **115**, 514–522.
137 A. S. Nizovtsev and S. G. Kozlova, *J. Phys. Chem. A*, 2013, **117**, 481–488.
138 A. S. Nizovtsev, *J. Comput. Chem.*, 2013, **34**, 1917–1924.
139 S. Berski, J. Andrés, B. Silvi and L. Domingo, *J. Phys. Chem. A*, 2003, **107**, 6014–6024.
140 V. Polo, J. Andres, R. Castillo, S. Berski and B. Silvi, *Chem. – Eur. J.*, 2004, **10**, 5165–5172.
141 J. C. Santos, V. Polo and J. Andrés, *Chem. Phys. Lett.*, 2005, **406**, 393–397.
142 L. R. Domingo, E. Chamorro and P. Perez, *Org. Biomol. Chem.*, 2010, **8**, 5495–5504.
143 I. Mbouombouo Ndassa, B. Silvi and F. Volatron, *J. Phys. Chem. A*, 2010, **114**, 12900–12906.
144 S. Berski and Z. Latajka, *Int. J. Quantum Chem.*, 2011, **111**, 2378–2389.
145 W. Benchouk, S. M. Mekelleche, B. Silvi, M. J. Aurell and L. R. Domingo, *J. Phys. Org. Chem.*, 2011, **24**, 611–618.
146 P. González-Navarrete, L. R. Domingo, J. Andrés, S. Berski and B. Silvi, *J. Comput. Chem.*, 2012, **33**, 2400–2411.
147 M. Rios-Gutierrez, P. Perez and L. R. Domingo, *RSC Adv.*, 2015, **5**, 58464–58477.
148 V. Polo, P. Gonzalez-Navarrete, B. Silvi and J. Andrés, *Theor. Chem. Acc.*, 2008, **120**, 341–349.
149 J. Contreras-García, A. Martín Pendás and J. M. Recio, *J. Phys. Chem. B*, 2008, **112**, 9787–9794.
150 M. R. Ryzhikov, V. A. Slepkov, S. G. Kozlova and S. P. Gabuda, *J. Comput. Chem.*, 2014, **35**, 1641–1645.
151 P. K. Chattaraj, P. Fuentealba, B. Gómez and R. Contreras, *J. Am. Chem. Soc.*, 2000, **122**, 348–351.
152 R. J. Gillespie, *Chem. Soc. Rev.*, 1991, **21**, 59–69.
153 A. Martín Pendás, E. Francisco and M. Blanco, *Chem. Phys. Lett.*, 2008, **454**, 396–403.
154 R. J. Gillespie, S. Noury, J. Pilmé and B. Silvi, *Inorg. Chem.*, 2004, **43**, 3248–3256.
155 A. Burkhardt, U. Wedig, H. G. von Schnering and A. Savin, *Z. Anorg. Allg. Chem.*, 1993, **619**, 437–441.
156 D. B. Chesnut, *J. Phys. Chem. A*, 2000, **104**, 11644–11650.
157 D. Wagman, W. Evans, V. Parker, R. Schumm, I. Halow, S. Bailey, K. Churney and R. Nuttall, *J. Phys. Chem. Ref. Data*, 1982, **11**, 1–392.
158 R. G. Parr, L. v. Szentpály and S. Liu, *J. Am. Chem. Soc.*, 1999, **121**, 1922–19246.
159 A. G. Girichev, N. I. Giricheva, N. Vogt, G. V. Girichev and J. Vogt, *J. Mol. Struct.*, 1996, **384**, 175–182.
160 G. Herzberg, *Molecular Spectra and Molecular Structure. II. Infrared and Raman Spectra of Polyatomic Molecules*, Van Nostrand, Princeton, 1945.
161 R. G. Bergman, *Acc. Chem. Res.*, 1973, **6**, 25–31.
162 M. N. Glukhovtsev, A. Pross, H. B. Schlegel, R. D. Bach and L. Radom, *J. Am. Chem. Soc.*, 1996, **118**, 11258–11264.
163 L. Joubert, M. Pavone, V. Barone and C. Adamo, *J. Chem. Theory Comput.*, 2006, **2**, 1220–1227.
164 G. A. Olah and P. Schilling, *J. Am. Chem. Soc.*, 1973, **95**, 7680–7686.
165 F. O. Rice and E. Teller, *J. Chem. Phys.*, 1938, **6**, 489–496.
166 G. S. Hammond, *J. Am. Chem. Soc.*, 1953, **77**, 334–338.
167 M. E. Alikhani, M. d. C. Michelini, N. Russo and B. Silvi, *J. Phys. Chem. A*, 2008, **112**, 12966–12974.
168 J. Andrés, S. Berski, L. R. Domingo, V. Polo and B. Silvi, *Curr. Org. Chem.*, 2011, **15**, 3566–3575.
169 A. Sánchez-Gonzéz, S. Melchor, J. A. Dobado, B. Silvi and J. Andrés, *J. Phys. Chem. A*, 2011, **115**, 8316–8326.
170 J. Andrés, S. Berski, L. R. Domingo and P. González-Navarrete, *J. Comput. Chem.*, 2012, **33**, 748–756.
171 J. Andrés, S. Berski, J. Contreras-García and P. González-Navarrete, *J. Phys. Chem. A*, 2014, **118**, 1663–1672.
172 S. Berski, A. J. Gordon and L. Z. Ciunik, *J. Mol. Model.*, 2015, **21**, 57.
173 S. Berski and L. Z. Ciunik, *Mol. Phys.*, 2015, **113**, 765–781.